ELSEVIER

Catalysis Today 53 (1999) 259–271

CATALYSIS TODAY

www.elsevier.com/locate/cattod

# Dynamic Monte-Carlo simulations of reactions in heterogeneous catalysis

A.P.J. Jansen [a,*], J.J. Lukkien [b]

[a] *Schuit Institute of Catalysis, T/SKA, Eindhoven University of Technology, P.O. Box 513, 5600 MB Eindhoven, The Netherlands*
[b] *Department of Mathematics and Computing Science, Eindhoven University of Technology, P.O. Box 513, 5600 MB Eindhoven, The Netherlands*

**Abstract**

Dynamic Monte-Carlo simulations form a powerful and easy-to-use tool to study the kinetics of reactions in heterogeneous catalysis. The simulations can be viewed as a numerical method to solve the Master Equation that describes the evolution of the catalyst's surface and the adsorbates, and which can be derived from first principles. The rate constants in this equation can be computed using quantum chemical methods. The Master Equation can also be used to derive the macroscopic reaction-rate equations, or reaction-diffusion equations. These equations are often convenient to interpret the results of the simulations. We show how various phenomena in heterogeneous catalysis (point defects, steps, surface reconstruction, lateral interactions, spatially varying surface composition) can be modeled. Numerous efficient algorithms have been developed for doing Dynamic Monte-Carlo simulations, and we discuss which one is the most appropriate for a given process that one wants to simulate. We also discuss some new developments that relate to simulating fast diffusion and large-scale pattern formation. 

## 1. Introduction

Although kinetics plays such an important role in catalysis, its theory has for a long time mainly been restricted to macroscopic rate equations. These implicitly assume a random distribution of adsorbates on the catalyst's surface. Effects of lateral interactions, reactant segregation, site blocking, and defects have only been described *ad hoc*. With the advent of dynamic Monte-Carlo simulations (DMC simulations), also called kinetic Monte-Carlo simulations, it has become possible to follow reaction systems on an atomic scale, and thus to study these effects.

The application of Monte-Carlo simulations to non-equilibrium reaction systems in heterogeneous catalysis took off properly only in 1986 with a paper by Ziff et al. on the lattice-gas version of a simple Langmuir–Hinshelwood model of CO oxidation on a transition metal surface [1]. (Equilibrium Monte-Carlo methods have been used, of course, much longer.) This model is nowadays often called the ZGB-model after the original authors. That paper discussed the first-order kinetic phase transition between the reactive phase and the phase with CO poisoning, and the continuous kinetic phase transition between the reactive phase and the phase with oxygen poisoning. Macroscopic rate equations predict the first-order transition at very different partial pressures than the simulations, and do not predict the continuous transition at all. The ZGB-model also

* Corresponding author. Tel.: +31-40-247-5037
*E-mail address:* tgtatj@chem.tue.nl (A.P.J. Jansen)

0920-5861/99/$ – see front matter 
PII: S0920-5861(99)00120-0

beautifully shows the effect of heterogeneity in the adlayer; because of the infinitely fast formation of $CO_2$, there is a segregation of the reactants in CO and oxygen islands. As the original ZGB-model is very simple (in particular, because of absence of CO diffusion the macroscopic rate equations are really closer to reality), it has later been extended and modified by numerous people to include desorption of the reactants, diffusion, an Eley–Rideal mechanism for the oxidation step, physisorption of the reactants, lateral interactions, an oxidation step with a finite rate constant, surface reconstruction, and additional poisoning adsorbates (see [2] for a discussion).

A large number of papers on Monte-Carlo simulations on other systems in heterogeneous catalysis soon followed. A good review on kinetics in catalysis that discusses these simulations is a paper by Lombardo and Bell [3]. In most of these papers the used DMC is presented intertwined with the simulated model resulting in an algorithmic description, in a similar way as in the paper by Ziff et al. [1]. The heart of this algorithm is the random selection of a site followed by the selection of a type of reaction. The latter selection is based on the chemical equations in the simulated system. The different rate constants of these reactions are included as probabilities for selection. This also implies that such a selection or trial sometimes results in no reaction occurring. The unit of time is the Monte-Carlo step which corresponds to one such a trial per site. The relation between a Monte-Carlo step and real time is not always made explicit but usually one Monte-Carlo step is $1/R$ on average, where $R$ is either the sum of the rate constants, or the maximum rate constant.

Presenting the simulation of a chemical system as an algorithm has the disadvantage that it is sometimes hard to recognize the original chemical equations and their rate constants. The constant of proportionality relating MC steps to time depends on the external conditions (e.g., temperature). If this constant is not given it is not possible to relate the simulation results directly to experiment.

A better way to start is to relate the rate constants directly to exponential distributions for occurrence times of reactions, as the algorithms mentioned above can be derived from this. The use of exponential distributions is implied by the classic work of Gillespie [4,5]. Binder gives a good introduction and several algorithms [6]. Using exponential distributions is correct if rate constants are truly constant but not when one wants to simulate, for example, temperature-programmed desorption experiments. Meng and Weinberg suggested in that case to assume that the rate constant are constant over small time intervals (equal to the exact value at the beginning of an interval), and that they change discontinuously from one interval to the next [7]. In the limit, for intervals small enough this is correct. However, if the intervals are too large, e.g., a temperature desorption experiment, this method systematically underestimates the rate constants.

The background of using the exponential distributions is a Master Equation (ME) that is often used in statistical physics for lattice-gas models. Based on this and on work by Gillespie on the use of Monte-Carlo methods to solve rate equations [4,5], we have developed a method which gives the correct time dependence even for systems with time-dependent rate constants [8]. Moreover, we could show that the ME can be derived from first principles, so that ab-initio kinetics is possible [9]. The use of the ME also has the advantage that it is very easy to make links with other theories of kinetics. Macroscopic rate equations can be derived from the ME as well. The derivation shows exactly on what approximations they are based, and suggests how these rate equations might be improved. More recently we have also developed new and more efficient algorithms for the simulations [10].

The purpose of this paper is not to present some new DMC algorithm or to discuss DMC simulations of a particular system, but to show that recent advances in theory and software have made DMC simulations a powerful and easy-to-use tool to study the kinetics of many systems in a way that would otherwise be infeasible. Among these are systems with time-dependent rate constants (temperature-programmed desorption and linear sweep voltammetry), and systems with lateral interactions. The contents of this paper is as follows. Section 2 presents the theory on which DMC simulations are based. We show that they are really part of a more encompassing theory of kinetics. Central in this theory is a ME that describes the evolution of a catalyst and its adsorbates. The parameters in this ME can be computed with ab-initio quantum chemical methods, so that we may speak of ab-initio kinetics. DMC simulations really form a method to solve the

ME exactly. Approximate methods to solve it lead, among others, to the conventional macroscopic rate equations and reaction-diffusion equations. We pay somewhat more attention than usual to the way we model a system, because, although this aspect often seems evident, it is really the reason why the DMC simulations can be applied to so many and such differing systems and phenomena. This point is expanded further in Section 3, in which we show a number of examples DMC simulations in practice. Finally, Section 4 discusses fast diffusion, often the bane of DMC simulations, and some new developments to handle it.

## 2. Theory

Three parts can be distinguished in our DMC method; the model representing the catalyst and the adsorbates, the ME that describes the evolution of the system, and the MC algorithms to solve the ME. In this paper we focus mainly on the model. The ME and the MC algorithms have been described extensively elsewhere [8,10,11]. The three contribute differently to making our DMC method worthwhile. The model insures that it is easy to study a very broad range of systems and phenomena. The ME forms the link with other kinetic theories like macroscopic rate equations and reaction-diffusion equations. As the parameters in the ME can be calculated using ab-initio quantum chemical methods, very similar to normal rate constants, it is the ME that allows us to talk about ab-initio kinetics. Finally, the MC algorithms make our DMC method extremely efficient.

### *2.1. The physical model*

For our model we assume that adsorption takes place at well-defined sites. These sites are represented by points. We will assume that these points form a regular grid, a lattice, although this is not strictly necessary. One can block this grid into unit cells and we admit the case with more than one grid point per unit cell (see Fig. 1). It is important to realize that, even though Fig. 1 may suggest otherwise, the model does not contain any information on the distance between the sites, or which sites are nearest neighbors, next-nearest neighbors, etc. As will be explained below, this kind in information is contained explicitly in the description of the reactions.

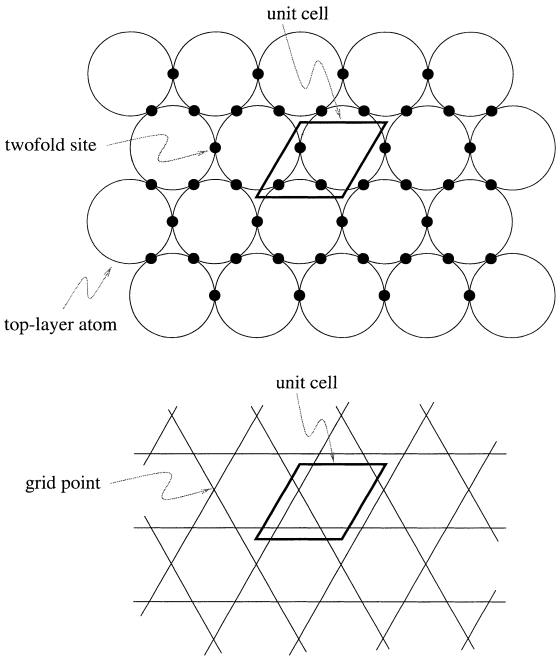


Fig. 1. An example of a grid (bottom) used in a dynamical Monte-Carlo simulation. The grid points correspond to two-fold sites on a (111) surface of a fcc metal (top).

A label is attached to each grid point. The most common use of this label is that it specifies the adsorbate at the site. (A special label is used for a vacant site.) Because of reactions, this implies that the labels will change during a simulation. Indeed, a simulation consists of nothing but changes of the labels according to reactions (see Fig. 2), and the determination of times when the reactions take place. The specification of a reaction consists of a set of grid points, labels attached to them corresponding to the adsorbates before the reaction has taken place (reactants), labels corresponding to the adsorbates after the reaction has taken place (products), and some rate constant. The set of grid points should be regarded as a representation for all sets of grid points where the reaction may occur. All these sets are related via translational symmetry and possibly (combinations with) rotations and reflections.

The use of labels need not be restricted to the specification of the adsorbate at a site. It may also tell something about the type of site. The examples below will show various instances of such usage.

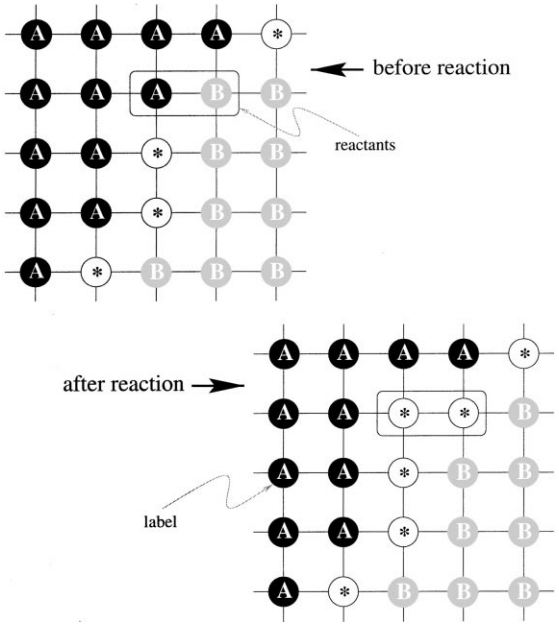


Fig. 2. Example of the use of labels in a model of a system with A(ads)+B(ads) $\rightarrow$ 2∗+AB(gas) reactions on a square grid. At the place where an island of A's and an island of B's touch (marked by the rectangle) an A reacts with a B to form two vacant sites. (Vacant sites are indicated by *.)

### 2.2. The master equation

The evolution of the adlayer and the substrate is described by the ME.

$$\frac{\mathrm{d}P_\alpha}{\mathrm{d}t} = \sum_\beta \left[ W_{\alpha\beta} P_\beta - W_{\beta\alpha} P_\alpha \right], \tag{1}$$

where $\alpha$ and $\beta$ refer to the configuration of the adlayer, the $P$'s are the probabilities of the configurations, $t$ is time, and the $W$'s are transition probabilities per unit time. These transition probabilities give the rates with which reactions change the occupations of the sites. They are very similar to reaction rate constants and we will use this term in the rest of this paper. $W_{\alpha\beta}$ corresponds to the reaction that changes $\beta$ into $\alpha$. A configuration can be regarded loosely as the way the adsorbates are distributed over all sites in the system. However, as labels may have a more general use, it is better to speak about a configuration being an assignment of labels to all grid points.

The ME has been used extensively in the statistical physics literature for the dynamics of all kinds of lattice-gas models. We would like to point out, however, that for reactions on surfaces this equation can be derived from first principles [11]. The derivation shows that the rate constants can be written as

$$W_{\alpha\beta} = \frac{k_\mathrm{B}T}{h} \frac{Q^\ddagger}{Q} \exp\left[ -\frac{E_\mathrm{bar}}{k_\mathrm{B}T} \right], \tag{2}$$

with $k_\mathrm{B}$ the Boltzmann-constant, $h$ Planck's constant, $T$ temperature, and $E_\mathrm{bar}$ the energy barrier of the reaction that transforms configuration $\beta$ into configuration $\alpha$. The partition function $Q^\ddagger$ and $Q$ can be interpreted as the partition functions of the transition state and the reactants, respectively, although there are some small, often negligible, differences [11]. This expression is, of course, familiar from Transition-State Theory (TST). Indeed, the derivation of the ME is very similar to Keck's derivation of the variational form of TST [12–14]. The important point is that the derivation of the ME from first principles makes an ab-initio approach to kinetics possible.

As we shall show, DMC is really nothing but a method to solve the ME, but it is not the only method that is possible. The ME also forms a link to other theories of kinetics; e.g., the rate equations that are normally used. Suppose we have a property $X$ of the system that has value $X_\alpha$ when the system is in configuration $\alpha$. Then the statistical average of $X$ is given by [11]

$$\langle X \rangle = \sum_\alpha P_\alpha X_\alpha. \tag{3}$$

The rate of change of $X$ is then given by

$$\frac{\mathrm{d}\langle X \rangle}{\mathrm{d}t} = \sum_\alpha \frac{\mathrm{d}P_\alpha}{\mathrm{d}t} X_\alpha = \sum_{\alpha\beta} W_{\alpha\beta} P_\beta \left[ X_\alpha - X_\beta \right]. \tag{4}$$

The right-hand-side of this expression is the statistical average of the change in $X$ in the reaction $\beta \rightarrow \alpha$ times the rate constant of that reaction. Rate equations for the coverages can be derived by taking for $X$ the number of atoms or molecules of a particular type.

Two examples should make this clear. Suppose that we have a simple desorption A(ads) $\rightarrow$ ∗ + A(gas), where A is the particle that desorbs, and * is a vacant site. With $\mathrm{A}_\alpha$ the number of A's in configuration $\alpha$ we have

$$\theta_\mathrm{A} = \frac{1}{S}\langle \mathrm{A} \rangle = \frac{1}{S} \sum_\alpha P_\alpha \mathrm{A}_\alpha, \tag{5}$$

with $S$ the number of sites in the system. The rate equation now becomes

$$\frac{d\theta_A}{dt} = \frac{1}{S}\sum_{\alpha\beta} W_{\alpha\beta} P_\beta \underbrace{[A_\alpha - A_\beta]}_{=0,-1}$$
$$= -\frac{1}{S} W_{des} \sum_\beta A_\beta P_\beta = -W_{des}\theta_A. \quad (6)$$

The expression in square brackets is 0 if the transition $\beta \to \alpha$ does not correspond to a desorption, and hence $W_{\alpha\beta} = 0$, and it is $-1$ otherwise. The factor $A_\beta$ results from the fact that there are so many terms in the summation over $\alpha$ for which $\beta \to \alpha$ does correspond to a desorption.

The derivation above is exact. In general, rate equations are based on the so-called mean-field approximation (MFA) [11]. When we have the reaction

A(ads) + B(ads) $\to$ 2 ∗ +AB(gas), then the exact expression

$$\frac{d\theta_A}{dt} = -W_{des}\, N_{AB} \quad (7)$$

contains the factor $N_{AB}$ that stands for the statistical average of the number of A–B pairs. The rate equation is obtained using $N_{AB} = Z\theta_A\theta_B$, where $Z$ is the coordination number of the grid ($Z = 4$ for a square grid, $Z = 6$ for a hexagonal grid, etc.). This approximation is based on the assumption that the A's and B's are randomly distributed over the substrate. This need not be the case, however.

### 2.3. The Monte-Carlo algorithms

The DMC simulations form a powerful numerical method to solve the ME exactly. In fact there are numerous DMC algorithms that might be used; a recent taxonomy of these algorithms contained no less than 48 [15]. Most of them are not efficient for any reaction system, however. For a general ME various algorithms have been given by Binder [6]. DMC algorithms for rate equations have even been given earlier by Gillespie [4,5]. Our work has mainly focussed on making these algorithms efficient for lattice-gas systems [8,10,15]. We will deal here only with the essential aspects, and we will point out the most important factors that determine the choice of the algorithm.

All DMC algorithms generate an ordered list of times at which a reaction takes place, and for each time in that list the reaction that occurs at that time. A DMC simulation starts with a chosen initial configuration. The list is traversed and changes are made to the configuration corresponding to the occurring reactions.

The method that is conceptually simplest is the First-Reaction Method (FRM) [4–6,8,10]. It can be applied to any system, but it may not be the most efficient method [15]. For each configuration that occurs a list of all possible reactions is computed, and for each reaction a time of occurrence is generated. If the rate constant is time independent and the current time is $t$, then the reaction $\beta \to \alpha$ will occur at time $t + \Delta t$ with $\Delta t = -(1/W_{\alpha\beta}) \ln r$, where $r$ is a random deviate of the unit interval [16]. The list of all reactions is ordered according to time of occurrence, and the configuration is changed corresponding to the first reaction in the list. This leads to a new configuration and a new time, and then the whole procedure is repeated. As the list of reactions does not have to be regenerated entirely after each configuration change, FRM is not as inefficient as it may seem. However, computer time per reaction does depend logarithmically on the number of sites in the system. This is because the list of reactions is implemented as a priority queue. Operations on it scale logarithmically with its size, [17] and the number of reactions, which is its size, is proportional to the size of the system. It can be shown that FRM generates configurations with probabilities that are solutions of the ME.

The reason for the logarithmic dependence on the system size in FRM is caused by updating the list of all reactions after each configuration change. We can do away with this list as follows. Instead of a time of occurrence of each reaction we generate only a time for the first reaction. If $W_k$ is the rate constant of a reaction of type $k$ (e.g., CO adsorption, $CO_2$ formation, etc.) and there are $N_k$ reactions of this type possible, then the first reaction will occur at time $t + \Delta t$ with $\Delta t = -(1/\sum_k N_k W_k) \ln r$. The type of this reaction is then randomly picked with probability proportional to $N_k W_k$ [4–6,8,10]. The actual reaction is determined via a random selection in a list of reactions of this type. In [10] it is shown that it is correct to maintain only an approximation of this list, which improves the performance of the algorithm significantly. Alternatively, the reaction can be determined by randomly looking

at the surface for a reaction of that type. Once this has been done a new configuration and a new time is obtained and the procedure is repeated. This method is called the Variable Time-Step Method (VSSM). An important property is that computer time per reaction does not depend on the system size.

A drawback of VSSM is that there is still some bookkeeping involved in the computation of the $N_k$'s. This can be avoided using oversampling [10]. The maximum number of reactions of type $k$ equals the number of sites $S$. (Here we consider reactions to belong to different types even if only the orientation of the sites involved is different.) The new time $t + \Delta t$ is generated using $\Delta t = -(1/S\sum_k W_k)\ln r$. Then the type of reaction is picked proportional to $W_k$, and one of the $S$ possible sites for the reaction is picked at random. If the reaction is possible there, then the configuration is changed accordingly. Otherwise, the configuration is not changed; only the time is updated. This method is called the Random-Selection Method (RSM) [10]. It is in fact the method used by Ziff et al. and others [1]. Its efficiency with respect to VSSM depends on the probability that a time update is accompanied by a configuration change. This probability should be large. When the number of sites involved in a reaction is large or when there are many reactions types, this probability is likely to be small, and RSM is not efficient. Yet another situation in which RSM is not efficient is discussed in the next paragraph.

It is possible to combine different DMC algorithms. For example, suppose that we have a system that is very efficiently simulated by RSM except for one reaction type, which would be well simulated by VSSM (Such a situation occurs when one has adsorption and an almost completely covered surface. RSM then works very poorly for adsorption, because there are only very few vacant sites where this reaction can take place). We determine a time $t_{\mathrm{RSM}}$ for all other reactions, and a time $t_{\mathrm{VSSM}}$ for the exceptional reaction type. If $t_{\mathrm{RSM}} < t_{\mathrm{VSSM}}$ one other reaction will occur first and the particular reaction will be determined as usual for RSM. If $t_{\mathrm{VSSM}} < t_{\mathrm{RSM}}$ an exceptional reaction will occur first and it will be determined as usual for VSSM. Similarly, other algorithms can be combined as well.

The expressions presented above to determine times of reactions are only for time-independent rate constants. With time-dependent rate constants the expressions become much more complicated. For temperature-programmed desorption and reaction experiments and for linear sweep voltammograms analytic expressions have been derived, [8,18] but that may not always be possible. In any case, it is much harder to determine the times of reactions if the rate constants are time dependent. This holds in particular if, as in VSSM and RSM, a time has to be determined for a set of reactions with different rate constants. Because FRM determines times for single reactions, which is much easier, it is the only algorithm that has so far been used in DMC simulations with time-dependent rate constants.

## 3. Examples

This section shows the practice of DMC simulations. As stated above, we will focus on how to model systems, and also on what one can get out of the simulations.

### *3.1. The Ziff–Gulari–Barshad-model with site blocking*

Labels are mainly used to indicate the adsorbate at a site. They may, however, also be used to specify a changed reactivity of a site. In fact, the difference in these ways to use the labels is really only in the interpretation. If a site becomes unreactive it can be labeled as such, but it may just as well be assumed that there is an adsorption of a unreactive species at that site. The Ziff–Gulari–Barshad-model (ZGB-model) with site blocking forms an example [19]. It can again be simulated efficiently using VSSM.

The ZGB-model is a lattice-gas version of the Langmuir–Hinshelwood-model of CO oxidation. The reactions are

$$\mathrm{CO(gas)} + * \rightarrow \mathrm{CO(ads)}, \tag{8}$$

$$\mathrm{O_2(gas)} + 2* \rightarrow 2\mathrm{O(ads)}, \tag{9}$$

$$\mathrm{CO(ads)} + \mathrm{O(ads)} \rightarrow \mathrm{CO_2(gas)} + 2*. \tag{10}$$

We have extended this model with slow reversible adsorption/desorption of an unreactive species.

$$\mathrm{X(gas)} + * \rightleftharpoons \mathrm{X(ads)}. \tag{11}$$

The only effect of this X is that it blocks sites so that CO and $O_2$ adsorption is suppressed. This causes

oscillations in the ZGB-model between a reactive and an unreactive state as follows.

In the reactive state there are many vacant sites, which are slowly being blocked by X's. The adsorption of CO decreases and $O_2$ adsorption decreases even more as two neighboring vacant sites are needed for the latter. At a critical coverage of X the reactive phase becomes unstable and the system jumps to an unreactive state in which the surface is almost completely covered by CO. In this situation the X's desorb. At another critical coverage of X the unreactive state becomes unstable and a fluctuation leading to two neighboring vacant sites allows a $O_2$ adsorption. Both adsorbed O's react yielding four vacant sites unto new $O_2$'s adsorb, etc. via an autocatalytic production of vacant sites the system goes back to the reaction state (see Fig. 3).

Permanent point defects can be treated very similarly. For example, CO adsorption at such a defect can be written as

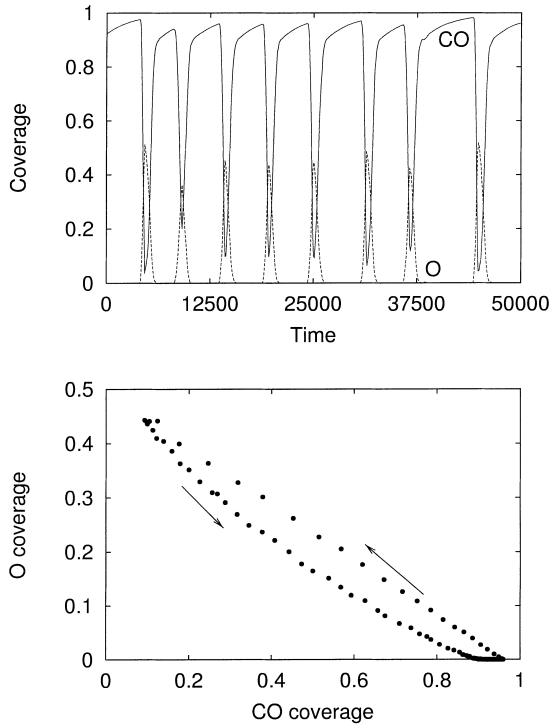


Fig. 3. Oscillations in the coverages (top) and the trajectory in phase space (bottom) for the ZGB-model with site blocking on a square grid of dimensions $256 \times 256$. The dots in the bottom plot are 30 time units apart.

$$\mathrm{CO(gas)} + *_{\mathrm{defect}} \rightarrow \mathrm{CO(ads)}_{\mathrm{defect}}. \quad (12)$$

The label at the site changes from $*_{\mathrm{defect}}$ to $\mathrm{CO}_{\mathrm{defect}}$. This change has, of course, a different rate constant from the normal CO adsorption. For steps labels may be used to distinguish between sites at the bottom of a step, at the top of a step, and on terraces. Other defects can be modeled likewise.

### 3.2. Surface reconstruction: CO oxidation on Pt(100)

The model of Gelten et al. to describe CO oxidation on Pt(100) is one of the most extensive models that have ever been used in DMC simulations [20]. In this process surface reconstruction plays an important role. A bare Pt(100) surface reconstructs to a quasi-hexagonal structure. Adsorption of CO lifts this reconstruction. The sticking probability of $O_2$ on the quasi-hexagonal structure is much smaller than on the unreconstructed surface, which results, once again, in oscillations, and, in our model, also in spatio-temporal pattern formation. There is a reactive state in which the surface is unreconstructed and there is CO and oxygen on the surface with many vacant sites. There is also an unreactive state with a reconstructed surface almost completely covered with CO and no oxygen. The transition between the states is caused by the slow changes in the surface. In the reactive state there are too few CO's and the surface reconstructs, suppressing $O_2$ adsorption. In the unreactive phase CO lifts the reconstruction making $O_2$ adsorption possible again.

Most other simulations on this system, either using a stochastic cellular automaton [21–24] or a dynamic Monte-Carlo approach as described above, [25–27] have concentrated on the reconstructions and the different sticking coefficients for oxygen. The simulations mainly differed in the way the reconstruction was modeled. The cells in the studies of Möller et al. and Wu and Kapral were allowed to represent more than one site/adsorbate [21,22]. The reconstruction depended in both studies on the state of a cell and its neighbors. Rosé et al. used a model describing the rearrangement of the substrate atoms during the reconstruction [23]. The work of Danielak et al. was a follow-up of the work of Wu and Kapral [24]. Vlachos et al. attributed the oscillations in the system not to the reconstructions, but to lateral interactions between the adsorbates [25]. The recent work of Kuzovkov

et al. concentrated on the effect that the different sticking coefficients of oxygen has on the kinetics, [26], whereas Kortlücke et al. not only discussed oscillations but also chaotic behavior [27]. Two important differences of these simulations with our work (the Gelten model) are the size of the system in the simulation, and the choice of the rate constants. We have found that nonlinear behavior often disappears when the system size is increased. We have therefore used grids at least of size $1024 \times 1024$. We have also tried to use literature data for the elementary reactions. This gives a more rigorous test for the correctness of the microscopic model when it is compared to experiments.

In our model of this system each unit cell has two labels. One label stands for the site and its adsorbate. The other label specifies whether the surface has reconstructed locally or not. This label is used to determine if oxygen can adsorb when the site is vacant. It is also used to determine the nearest neighbors of the site. If it indicates that there is no reconstruction, then it is assumed that the surface is locally square with the site having four nearest neighbors. If it indicates that there is a reconstruction, then the surface is locally hexagonal with the site having six nearest neighbors. The model has been simulated with a combination of VSSM and RSM.

To find oscillations in the coverages or the $CO_2$ formation it is necessary that many sites oscillate in phase. This means that there must be some synchronization mechanism. For the model of CO oxidation on Pt(100) this mechanism consists of circular reaction fronts in the reactive state. These reaction fronts move outwards and annihilate each other when they collide, leading to the unreactive state. As in this unreactive state the system is homogeneous, especially if CO is allowed to diffuse, the phase of the oscillations is fixed over the whole surface. The reaction fronts form a so-called cellular pattern (see Fig. 4). Depending on reaction conditions other spatio-temporal patterns can be formed as well, but then no oscillations are found.

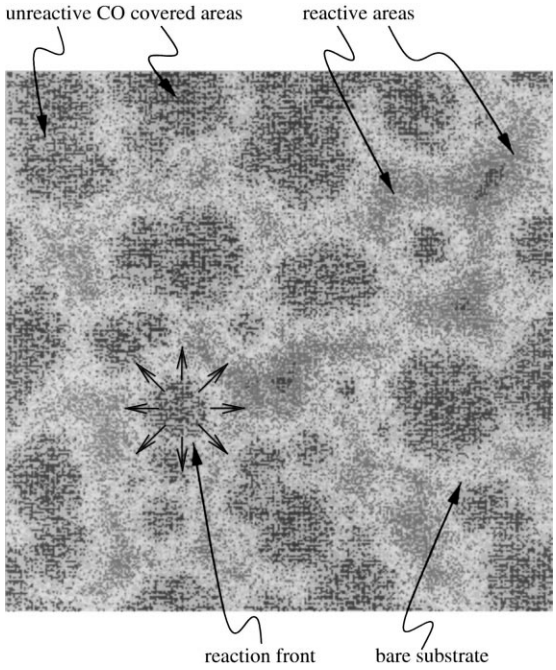


Fig. 4. A typical example of a cellular pattern that is formed in a simulation with a $1024 \times 1024$ grid in the model of CO oxidation on Pt(100) developed by Gelten et al. The regions with bare substrate are reconstructed to the quasi-hexagonal structure. The areas covered almost completely by CO and the reactive areas are non-reconstructed.

### *3.3. Bimetallic surfaces: CO electrooxidation on Pt–Ru electrodes*

Bimetallic surfaces can be modeled by having the label indicate both the adsorbate and the metal unto which it has adsorbed. This is similar to the CO adsorption on a point defect in Section 3.1. Alternatively, a different label can be used for the surface as in the case with surface reconstruction above.

CO electrooxidation on Pt–Ru electrodes is currently of much interest in electrocatalysis as the bimetallic system shows a higher reactivity than each of its constituents. Experiments indicate that dissociative adsorption of water on Ru, forming OH, occurs at a lower potential than on Pt, but the formation of $CO_2$ occurs at a lower potential on Pt. We have recently shown that a synergic effect occurs when the $CO_2$ formation taking place at the Pt–Ru interface is at least as fast as on Pt [28]. There should also be reasonably fast CO diffusion as otherwise CO on Pt will have to react with an OH also on Pt, which adsorbs only at a high potential (see Fig. 5). For this system FRM is used; the rate constants are written as

$$W = \nu \exp\left[-\frac{E_{\mathrm{act}}}{k_{\mathrm{B}}T}\right], \tag{13}$$

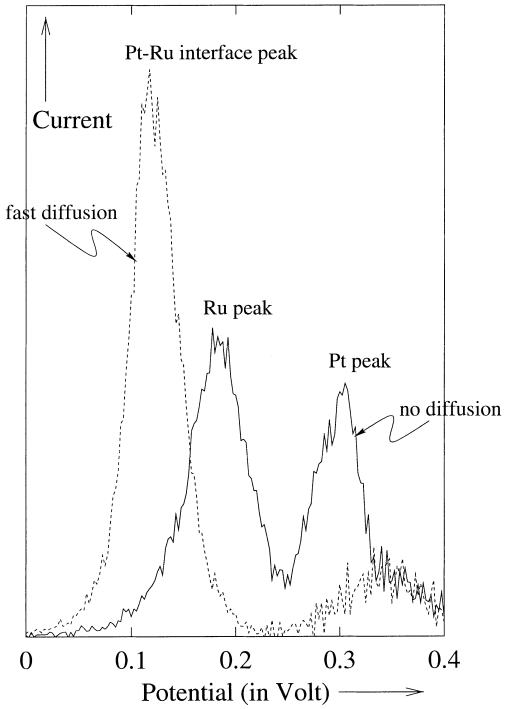


Fig. 5. Voltammogram of CO electrooxidation on a Pt–Ru electrode. The substrate consists of equal amounts of Pt and Ru sites, which are clustered in islands of the order of 1000 sites. The substrate is initially (at low potential) for 99% covered by CO. The potential is increased with a rate of 50 mV/s. Without CO diffusion the oxidation takes place in the Pt and Ru islands. With fast CO diffusion the oxidation takes place at the Pt–Ru interface. OH never diffuses.

and they are time dependent, as the activation energy $E_{\mathrm{act}}$ varies with the potential.

An interesting question is what the optimal structure is of the substrate. As $CO_2$ is mainly formed at the Pt–Ru interface, it seems reasonable to suppose that a checkerboard structure is best. This is indeed the case if there are equal numbers of Pt and Ru sites, but in general this is not the case. Suppose water adsorbs only on Ru, and CO adsorbs only on Pt. If the adsorption of water is much slower than all other reactions, then it is better to optimize this reaction by increasing the Ru content. We find that the optimal structure is a $\sqrt{5} \times \sqrt{5}$ structure with 80% Ru and 20% Pt (see Fig. 6). For different ratios of the rate constants yet other structures will be optimal [29].

### *3.4. Lateral interactions: NO reduction on Rh(111)*

A Rh(111) surface is prepared with 68% NO at low temperature. In a TPD experiment the temperature is raised with 5 K/s. The following reactions take place [30].

$$\mathrm{NO(ads)} + * \rightarrow \mathrm{N(ads)} + \mathrm{O(ads)}, \tag{14}$$

$$\mathrm{NO(ads)} \rightarrow \mathrm{NO(gas)} + *, \tag{15}$$

$$2\mathrm{N(ads)} \rightarrow \mathrm{N_2(gas)} + 2*, \tag{16}$$

$$2\mathrm{O(ads)} \rightarrow \mathrm{O_2(gas)} + 2*. \tag{17}$$

Besides these reactions, we also have surface diffusion of the adspecies.

The experimental results have two remarkable characteristics [31–34]. First, NO dissociation that is known to start around 275 K is postponed until NO desorption starts around 400 K. Around 450 K a sharp

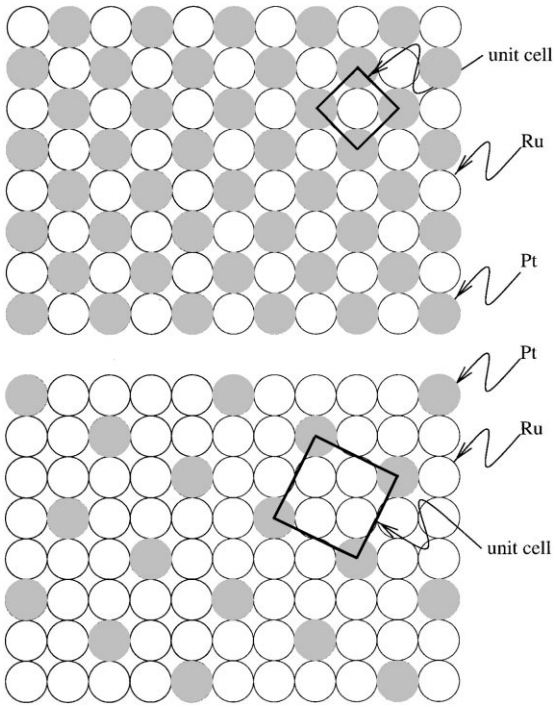


Fig. 6. Structures for CO electrooxidation on a Pt–Ru (100) surface when it is assumed that water adsorbs only on Ru and CO adsorbs only on Pt. The top structure is the optimal structure when the rate constants for water and CO are equal. The bottom structure is the optimal structure when water adsorption is much slower than CO adsorption.

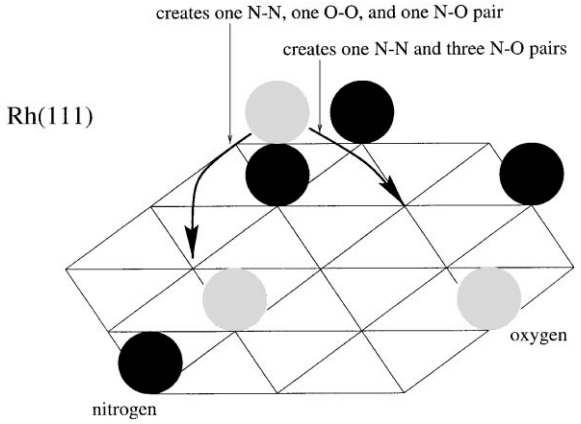


Fig. 7. We assume that adsorption on Rh(111) is on hollow sites; either fcc-sites or hcp-sites, but not both. We can therefore model the adsorption sites with a hexagonal lattice. Dissociation of NO to several different neighboring sites is possible. Besides introducing an N–O pair resulting from the occurrence of the reaction itself, the number of NO–NO, NO–N, NO–O, N–N, and O–O pairs on the surface may change depending on the occupation of neighboring sites.

$N_2$ desorption peak is observed, whereas this desorption is expected to start around 550 K. In both effects, lateral interaction is assumed to play a dominant role. The adspecies on neighboring sites of the two sites involved in the reaction are assumed to have a strong influence on the speed of the reaction. This can be explained through the observation that occurrence of, e.g., a dissociation decreases the number of NO–X pairs and increases the number of N–X and O–X pairs on the surface, where X is an arbitrary adsorbate (see Fig. 7). We therefore model the lateral interaction as a change in the activation energy of the reaction (see Eq. (13)). This change is based on the difference in (lateral) energy between the states before and after the reaction. For the discussion we restrict ourselves to interaction of neighboring pairs and, hence, the total lateral energy of a particle or pair of particles is given by the sum of the contributions of the neighbors. The change in activation energy is then given by a Brønsted relation.

$$E_a' = E_a + \alpha \Delta E_L \tag{18}$$

Here, $E_a$ is the activation energy without lateral interaction, $E_a'$ is the activation energy with lateral interactions, $\alpha \in [0, 1]$ is the Brønsted coefficient and $\Delta E_L$ is the difference in lateral energy, before and after the reaction. For the reaction in the reverse direction (if included in the model) a Brønsted coefficient of $1 - \alpha$ is used.

If we model lateral effects through patterns as we did until now, we end up with $4^8$ patterns involving the eight neighboring sites of the reacting pair. This is unfortunate because after execution of a reaction a lot of pattern matching is necessary to determine the new reactions that have become possible. Hence, rather than using pattern matching, we compute the effective activation energy of newly enabled reactions through inspection of the neighborhood of the reacting sites. Although this is far more effective than using pattern matching, simulations with lateral interaction are significantly slower. This is because a reaction rate changes (and a new time has to be recomputed) any time that a change occurs in the neighborhood contributing to the lateral interaction. This is simply an effect of using large neighborhoods and cannot be avoided. Because the rate of a reaction varies significantly depending on the neighborhood we use FRM as the simulation method. (Remember that in FRM, times are computed for each individual reaction. VSSM and RSM rely on representing all different rate constants. Due to the large number of patterns, and hence different rate constants, this is not feasible.)

In the model that we built we assumed strong lateral repulsive interactions between NO and N, NO and O, N and N. The result was in good agreement with the experimental findings demonstrating that this way of modeling is indeed viable.

## 4. New developments

The hardest part for a DMC simulation is diffusion. In principle, diffusion is simulated just as any (other) reaction. The problem is that there are situations where the rate constant for diffusion is much larger than those for the other reactions, and diffusion has no negative feedback that reduces the number of reactions/hops. This has two consequences. First, most of the computer time will be spent on the diffusion. There will be few other reactions and the statistics of these, which are often the more interesting ones, will be bad. Second, if the adsorbates form patterns, then the size of them depends on the diffusion rate; fast diffusion means large patterns. Consequently a large

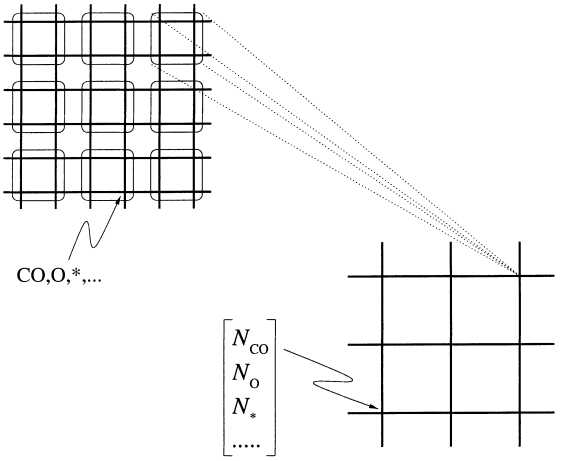


Fig. 8. An example of a blocking transformation for a model of CO oxidation. Here blocks of $2 \times 2$ grid points are used. The label of a point on the original grid corresponds to the adsorbate at that position. The label of a point on the new grid corresponds to the number of adsorbates in the corresponding block.

system needs to be used in the simulation, which may not be feasible.

A possible solution to this problem is to change the model of the system. Instead of a grid with each grid point corresponding to a single site, we may have each grid point corresponding to a (large) block of sites (see Fig. 8). This obviously can solve the size problem. The new grid points are labeled with the number of adsorbates in the block. This solves the problem with the diffusion for the following reasons. First, diffusional hops within the blocks can be ignored, because they do not change the number of adsorbates within a block. If each grid point corresponds to a block of $L \times L$ sites, then only hops from the sites at the border of the block into neighboring blocks have to be taken into account. If the grid is square this involves $4L$ out of $4L^2$ possibilities for hops from an arbitrary site in the block, thus reducing the number of hops that have to be simulated by a factor of $L$. The rate constant for the hops has to be changed as well, because the distance between grid points is $L$ times the distance between sites. Suppose we have a single particle on a square grid and $L \times L$ blocks. The diffusion constant is proportional to the square of the distance between grid points, so that an increase of this size by a factor $L$ has to be compensated by a factor $1/L^2$ in the rate of the hops. There is already a reduction by a factor $L$, because the particle has to be at one of $L$ border sites to hop to a particular neighboring block, and the probability to find the particle there is $1/L$. (This reduction factor $L$ is the same as the one in the number of hops that have to be simulated.) To get the same diffusion constant the rate constant for the hops then has to be reduced by a further factor $L$. The total reduction of the amount of computer time spent on diffusion is therefore a factor $L^2$.

In the absence of lateral interaction, diffusion mixes the adsorbates. The simplest case is then that within a block all adsorbates are distributed randomly, so that a MFA may be used for the kinetics within a block. This can be incorporated in a DMC simulation [4,5,35,36]. For moderately fast diffusion this solves all problems. For example, if there are $N_A$ A's in a block, then the rate constant for A desorption in that block is increased by a factor $N_A$. If there are $N_A$ A's and $N_B$ B's, then the rate constant for a A + B reaction is increased by the number of AB pairs, which equals $4(L-1)N_A N_B/L^3$ for a square grid and a block of size $L \times L$ with well-mixed adsorbates. One can determine similar expressions for reactions that occur on the boundary of two blocks. Note that, although blocking reduces the number of hops that have to be simulated, the number of other reactions in the simulation remains same.

If diffusion is very fast, then the size of the system and the number of sites and adsorbates may become so large that there are too many reactions for a simulation to be feasible. This problem may be solved by replacing the adsorbates in a block by a smaller number of fictitious adsorbates. For example, if the number of A's in a block is $N_A$, then, instead of these $N_A$ A's, we assume that there are only $\tilde{N}_A \equiv f N_A$ $\tilde{A}$'s in the block with $f \ll 1$. The coverage of A in the block should, of course, be corrected by this factor $f$; i.e., $\theta_A = \tilde{N}_A/(fL^2)$. It may seem that reactions that change the number of these new $\tilde{A}$'s cause too large changes in the coverage. It can be shown that this is not the case for unimolecular reactions, because the rate of these reactions is proportional to the number of reactants. Suppose that we have A desorption with rate constant $W_{des}$. This gives us

$$\frac{dN_A}{dt} = -W_{des} N_A, \tag{19}$$

for the change of the number of A's in a block. In

terms of $\tilde{A}$'s we have

$$\frac{d\tilde{N}_A}{dt} = -\tilde{W}_{des}\tilde{N}_A, \tag{20}$$

where $\tilde{W}_{des}$ is the rate constant for desorption of $\tilde{A}$'s. Because this is a linear equation, both equations are consistent if $\tilde{W}_{des} = W_{des}$.

For bimolecular reactions the rate constant must be multiplied by the factor $f$. Suppose that we have a reaction A(ads) + B(ads) $\rightarrow 2* +$AB(gas) with rate constant $W_{rx}$. Then

$$\frac{dN_A}{dt} = -W_{rx}\frac{4(L-1)}{L^3}N_A N_B, \tag{21}$$

in an $L \times L$ block of a square grid. In terms of $\tilde{A}$'s and $\tilde{B}$'s we have

$$\frac{d\tilde{N}_A}{dt} = -\tilde{W}_{rx}\frac{4(L-1)}{L^3}\tilde{N}_A\tilde{N}_B. \tag{22}$$

With $\tilde{N}_A = fN_A$ and $\tilde{N}_B = fN_B$ we see that we must have $\tilde{W}_{rx} = W_{rx}/f$.

We see then that we have a reduction of the computer time spent on bimolecular reactions by a factor $f^2$. One factor $f$ arises, because the number of reactions is reduced, and one factor $f$ arises, because of the reduced rate constant. For unimolecular reactions the computer time is reduced only by a factor $f$, because the number of particles is reduced.

If there is some reason why the assumption of well-mixed adsorbates within a block is not correct, e.g., when there are lateral interactions, the situation is more difficult. There is no difference for reactions like simple desorption, A(ads) $\rightarrow * +$ A(gas), but for a bimolecular reaction like A(ads) + B(ads) $\rightarrow 2* +$AB(gas) difference is there. The problem is that we need to know the number of AB pairs within blocks and on boundaries of two blocks as a functions of the number of A's and B's within blocks. The Mean-Field expressions above are no longer correct. Better approximations, like the quasi-chemical approximation, [37] might be used, however. As the methods of this section have only been used in test cases, future studies will have to show if they are really viable.

## Acknowledgements

We would like to thank Profs. P.A.J. Hilbers and R.A. van Santen and Drs. M.T.M. Koper, R.J. Gelten and J.P.L. Segers (all of the Eindhoven University of Technology) for many stimulating discussions. We would particularly like to think Dr. Gelten for the providing Fig. 4 and Dr. Koper for Fig. 5. We would also like to thank Drs. J.W. Niemantsverdriet, M.J.P. Hopstaken, (both of the Eindhoven University of Technology) R.M. van Hardeveld (Shell), and H.J. Borg (Philips) for suggesting the work on NO reduction on Rh(111). This work has been performed under the auspices of NIOK, the Netherlands Institute for Catalysis Research, Lab Report No. TUE-99-5-99.

## References

[1] R.M. Ziff, E. Gulari, Y. Barshad, Phys. Rev. Lett. 56 (1986) 2553.
[2] R.M. Nieminen, A.P.J. Jansen, Appl. Catal. A: General 160 (1997) 99.
[3] S.J. Lombardo, A.T. Bell, Surf. Sci. Rep. 13 (1991) 1.
[4] D.T. Gillespie, J. Comput. Phys. 22 (1976) 403.
[5] D.T. Gillespie, J. Phys. Chem. 81 (1977) 2340.
[6] K.Binder, Monte Carlo Methods in Statistical Physics, Springer, Berlin, 1986.
[7] B. Meng, W.H. Weinberg, J. Chem. Phys. 100 (1994) 5280.
[8] A.P.J. Jansen, Comput. Phys. Comm. 86 (1995) 1.
[9] A.P.J. Jansen, J. Molec. Catal. A 119 (1997) 125.
[10] J.J. Lukkien, J.P.L. Segers, P.A.J. Hilbers, R.J. Gelten, A.P.J. Jansen, Phys. Rev. E 58 (1998) 2598.
[11] R.J. Gelten, R.A. van Santen, A.P.J. Jansen, Dynamic Monte Carlo Simulations of Oscillatory Heterogeneous Catalytic Reactions, in Molecular Dynamics, in press.
[12] J.C. Keck, J. Chem. Phys. 32 (1960) 1035.
[13] J.C. Keck, Discuss. Faraday Soc. 33 (1962) 173.
[14] J.C. Keck, Adv. Chem. Phys. 13 (1967) 85.
[15] J.P.L. Segers, Algorithms for the Simulation of Surface Processes, Ph.D. Thesis, Eindhoven University of Technology, 1999.
[16] W.H. Press, A. Teukolsky, W.T. Vetterling, B.P. Flannery, Numerical Recipes in C: The Art of Scientific Computing, Cambride University Press, Cambridge, 1992.
[17] D.E. Knuth, The Art of Computer Programming, Sorting and Searching, vol. 3, Addison-Wesley, Reading. MA, 1973.
[18] M.T.M. Koper, J.J. Lukkien, A.P.J. Jansen, P.A.J. Hilbers, R.A. va Santen, J. Chem. Phys. 109 (1998) 6051.
[19] A.P.J. Jansen, R.M. Nieminen, J. Chem. Phys. 106 (1997) 2038.
[20] R.J. Gelten, A.P.J. Jansen, R.A. van Santen, J.J. Lukkien, J.P.L. Segers, P.A.J. Hilbers, J. Chem. Phys. 108 (1998) 5921.

[21] P. Möller, K. Wetzl, M. Eiswirth, G. Ertl, J. Chem. Phys. 85 (1986) 5328.
[22] X.-G. Wu, R. Kapral, Physica A 188 (1992) 284.
[23] H. Rosé, H. Hempel, L. Schimansky-Geier, Physica A 206 (1994) 421.
[24] R. Danielak, A. Perera, M. Moreau, M. Frankowicz, R. Kapral, Physica A 229 (1996) 428.
[25] D.G. Vlachos, L.D. Schmidt, R. Aris, J. Chem. Phys. 93 (1990) 8306.
[26] V.N. Kuzovkov, O. Kortlücke, W. von Niessen, J. Chem. Phys. 108 (1998) 5571.
[27] O. Kortlücke, V.N. Kuzovkov, W. von Niessen, Phys. Rev. Lett. 81 (1998) 2164.
[28] M.T.M. Koper, J.J. Lukkien, A.P.J. Jansen, R.A. van Santen, A Lattice-Gas Model for CO Electrooxidation on Pt–Ru Bimetallic Surfaces, in J. Phys. Chem., in press.
[29] C. Hermse, 1999, private communication.
[30] V.P. Zhdanov, B. Kasemo, Surf. Sci. Rep. 29 (1997) 31.
[31] H.J. Borg, J.F.C.-J.M. Reijerse, R.A. van Santen, J.W. Niemantsverdriet, J. Chem. Phys. 101 (1994) 10052.
[32] R.M. van Hardeveld, Elementary Reactions in the Catalytic Reduction of NO on Rhodium Surfaces, Ph.D. Thesis, Eindhoven University of Technology, 1997.
[33] A.G. Makeev, M.M. Slinko, N.M.H. Janssen, P.D. Cobden, B.E. Niewenhuys, J. Chem. Phys. 105 (1996) 7210.
[34] A.G. Makeev, N.M.H. Janssen, P.D. Cobden, M.M. Slinko, B.E. Nieuwenhuys, J. Chem. Phys. 107 (1997) 965.
[35] M. Tammaro, J.W. Evans, J. Chem. Phys. 108 (1998) 762.
[36] T. Fricke, D. Wendt, Int. J. Mod. Phys. C 6 (1995) 277.
[37] V.P. Zhdanov, Elementary Physicochemical Processes on Solid Surfaces, Plenum Press, London, 1991.